

Simulation of mold filling and prediction of gas entrapment on practical high pressure die castings

ZHAO Hai-dong(赵海东), BAI Yan-fei(白砚飞), OUYANG Xiao-xian(欧阳晓贤), DONG Pu-yun(董普云)

State Engineering Research Center for Metallic Materials Net-shape Forming,
South China University of Technology, Guangzhou 510640, China

Received 13 October 2009; accepted 20 July 2010

Abstract: Element parameters including volume filled ratio, surface dimensionless distance, and surface filled ratio for DFDM (direct finite difference method) were proposed to describe shape and location of free surfaces in casting mold filling processes. A mathematical model of the filling process was proposed specially considering the mass, momentum and heat transfer in the vicinity of free surfaces. Furthermore, a method for gas entrapment was established by tracking flow of entrapped gas. The model and method were applied to practical ADC1 high pressure die castings. The gas entrapment prediction was compared with the fraction and maximum size of porosities in the different casting parts. The comparison shows validity of the proposed model and method. The study indicates that final porosities in high pressure die castings are dependent on both gas entrapment during mold filling process and pressure transfer within solidification period.

Key words: high pressure die casting; mold filling; gas entrapment

1 Introduction

Computer simulation of casting mold filling has been used by engineers to evaluate and optimize geometry design of castings and dies (or molds) as well as casting processing parameters. High pressure die casting process is a kind of net-shape processing method and is being widely used in making automotive components of Al, Mg and Zn alloys. In the process, liquid melt is injected into the die cavity, and flows with high velocity commonly over 10 m/s through ingates. The flow is turbulent in nature and usually causes entrapment of gas in die cavity, inducing porosities in final castings which are often detrimental to the casting mechanical properties[1–5] and are a very frequent reason for the casting rejection[6]. Simulation of the mold filling and prediction of gas entrapment can provide important and valuable information for optimization in die design and process parameter selection to avoid the rejection. Some recent researches proposed some methods to simulate the gas entrapment in the filling process[7–11]. However, the computer simulation application and validation with

quantitative porosity data on practical castings have not been reported to date, which are important to evaluate the simulation validity and to realize factors affecting the porosity formation.

In this study, using element parameters to describe the shape and location of free surfaces are proposed in modeling of mold filling with DFDM, and then a mathematical model of the filling process is established specially considering the mass, momentum and heat transfer in the vicinity of free surfaces. Also a method for predicting gas entrapment is founded by tracking flow of the entrapped gas. The model and method are applied to practical ADC1 high pressure die castings. The results are compared with experimentally analysis, and the comparison is discussed further.

2 Mathematical model

2.1 Mold filling

To describe free surfaces in the simulation of mold filling, the surfaces are simplified and treated as being parallel to the six surfaces of DFDM elements as shown in Fig.1, and the following elementary parameters are

Foundation item: Project(50975093) supported by the National Natural Science Foundation of China; Project(08-0209) supported by New Century Excellent Talent in University, Ministry of Education, China; Project(2009ZM0283) supported by the Fundamental Research Funds for the Central Universities, China

Corresponding author: ZHAO Hai-dong; Tel: +86-20-87112933; E-mail: hdzhao@scut.edu.cn
DOI: 10.1016/S1003-6326(09)60418-0

defined[12–13].

1) Volume filled ratio β_V : fraction of volume filled by liquid melt in the elements.

2) Surface dimensionless distance $\beta_{D,k(k=1-6)}$: ratio of the distance from simplified free surface to element surface to the length of element in corresponding direction. The distance may be solved according to the liquid flow through the element surfaces and the following equation:

$$1 - \beta_V = (1 - \beta_{D,1} - \beta_{D,2})(1 - \beta_{D,3} - \beta_{D,4}) \cdot (1 - \beta_{D,5} - \beta_{D,6}) \quad (1)$$

3) Surface filled ratio $\beta_{S,k(k=1-6)}$: fraction of area filled by liquid melt on the element surfaces. The ratios of full-filled and un-filled (empty) elements are set to 1 and 0, respectively, while for the partial-filled elements, the ratios are calculated based on $\beta_{D,k}$.

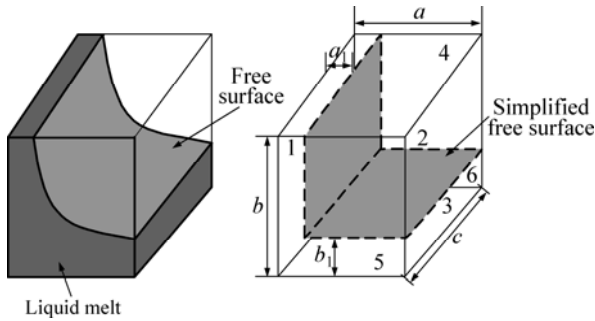


Fig.1 Schematics of description of free surfaces

Neglecting the density change of liquid melt during mold filling, the mass transfer during mold filling simulation with DFDM may be described by

$$\rho_L V_i (\beta_{V,i}^{t+\Delta t} - \beta_{V,i}^t) = \rho_L \sum_{k=1,6} (S_k \beta_{S,k}^{t+\Delta t} \mathbf{m}_k^{t+\Delta t}) \Delta t \quad (2)$$

where ρ_L is the density of liquid melt; V is the volume of element and subscript i is the number of the element; superscript t and $t+\Delta t$ are the simulation times; S is the area of the DFDM element surfaces and subscript k indicates the number of the surfaces; \mathbf{n} is the normal vector of liquid flowing through the surfaces; \mathbf{u} is the velocity of liquid melt flowing through the element surfaces; Δt is the time step.

Considering the momentum transfer with free surface elements, the momentum conservation of both full-filled and free surface elements can be calculated as

$$\rho_L (\beta_{D1,k} V_1 + \beta_{D2,k} V_2) \frac{u^{t+\Delta t} - u^t}{\Delta t} = M_c + M_v + M_g + M_p \quad (3)$$

where u is the velocity of liquid melt flowing through full-filled surfaces between two DFDM elements; $\beta_{D1,k}$ and $\beta_{D2,k}$ are the surface dimensionless distances of the two elements with respect to the surface, respectively; V_1

and V_2 are the volumes of two elements, respectively; M_c , M_v , M_g , and M_p are momentum terms of convection, viscosity, gravity and pressure, respectively. They may be calculated with

$$M_c = \sum_{j=1,6} (\rho_L u_j^t S_j u^t) \quad (4)$$

$$M_v = \mu \sum_{j=1,6} (S_j \frac{u_j^t - u^t}{d_j}) \quad (5)$$

$$M_g = -\rho_L (\beta_{D1,k} V_1 + \beta_{D2,k} V_2) \mathbf{g} \quad (6)$$

$$M_p = S(p_1^t - p_2^t) \quad (7)$$

where S_j expresses the area of the six surfaces of the dashed line box in Fig. 2 and subscript j indicates the number of the surfaces; u_j is the velocity of liquid flowing through the surfaces; μ is the viscosity; u_j expresses the distance of the surface to the central point of the shaded surface in Fig.2; \mathbf{g} is the gravity acceleration; S is area of the shaded surface in Fig.2; p_1 and p_2 are the metallic pressure in the two elements, respectively. The velocity of liquid melt flowing through the partial-filled surface is set to the average velocity of next full-filled neighbor surfaces.

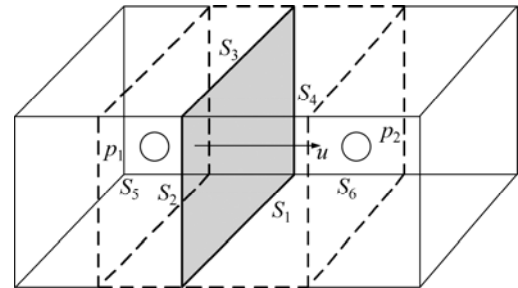


Fig.2 Schematics of momentum transfer of mold filling simulation

During the mold filling process, the temperature change in the liquid caused by the flow and heat transfer are governed by

$$\rho_L c_L V_i \beta_{V,i}^{t+\Delta t} \frac{T_i^{t+\Delta t} - T_i^t}{\Delta t} = \sum_{k=1,6} (S_k \beta_{S,k}^t \frac{T_{i,k}^t - T_i^t}{R_{i,k}}) + \sum_{k=1,6} [\rho_L c_L S_k \beta_{S,k}^{t+\Delta t} \mathbf{u}_k^{t+\Delta t} (T_{i,k}^t - T_i^t)] \quad (8)$$

where c_L is the specific heat capacity of liquid melt; T_i and $T_{i,k}$ are temperature of element i and its neighbor elements (including mold elements); $R_{i,k}$ is the heat conductivity resistance between element i and its neighbor elements; u is the velocity of liquid metal flowing into element i through the surfaces (or the second term on right hand is zero).

The heat transfer in the mold elements and between the liquid melt and mold is calculated with

$$\rho_M c_M V_i \frac{T_i^{t+\Delta t} - T_i^t}{\Delta t} = \sum_k (S_k \frac{T_{i,k}^t - T_i^t}{R_{i,k}}) + \sum_k (S_k \beta_{S,k}^t \frac{T_{i,k}^t - T_i^t}{R_{i,k}}) \quad (9)$$

where ρ_M and c_M are the density and specific heat capacity of mold materials, respectively; V is the volume of the mold element and subscript i is the number of the element; S is the area of the surfaces of element i and subscript k indicates the number of the surfaces; T_i and $T_{i,k}$ are the temperature of the element and its neighbor elements (including liquid melt elements); $R_{i,k}$ is the heat conductivity resistance between element i and its neighbor elements. The first term in right hand is the energy transfer of the element i with its neighbor mold elements, while the second one is the energy transfer of the element with liquid melt element.

2.2 Prediction of gas entrapment

In predicting the entrapment of cavity gas, the following is assumed in the present analysis: 1) the gas in a cavity is an ideal one; 2) pressure, temperature and density of gas in the cavity are constant in each gas group. The mass balance equation in the mold cavity can be written as[9]:

$$\frac{\rho_{ig}^{t+\Delta t} V_{ig}^{t+\Delta t} - \rho_{ig}^t V_{ig}^t}{\Delta t} = - \sum_j (n_{ij} S_{ij} u_{out}^{t+\Delta t} \rho^t) \quad (10)$$

$$u_{out}^{t+\Delta t} = K(p_{ig}^{t+\Delta t} - p_{air}^{t+\Delta t}) \quad (11)$$

where subscript ig is the number of gas group, ρ_{ig} the density of gas group, V_{ig} the volume of gas group, S_{ij} the surface between element i and j , u_{out} the velocity in air vent, ρ the density of gas, and K the flow conductance of gas in vent or ejector pin.

The pressure of the ideal gas can be written as:

$$p_{ig}^{t+\Delta t} = \frac{RT_{ig}}{M} \rho_{ig}^{t+\Delta t} \quad (12)$$

where M is the mass of the molecular, R the gas constant, T_{ig} the gas temperature, and p_{ig} the pressure.

The backpressure is used as the boundary pressure for solving flow field with Eq.(3) at each time step.

Therefore, the filling of liquid melt and gas escape as well as entrapment is coupled.

3 Simulation application and validation

Fig.3(a) shows the component of practical ADC1 high pressure die casting used in the brake system of high velocity railways, and Fig.3(b) presents geometry model used in the current simulation. The casting system includes three movable dies. In the simulation, total 12 096 000 cubic meshes of 0.8 mm×0.8 mm×0.8 mm are used. To consider gas flowing out of the die cavity and effect of cavity gas backpressure, the vents are set on the parting lines of the dies and overflows as shown in Fig.3(b). The thermal-physical data for the casting and dies are shown in Table 1. The boundary condition is set to velocity boundary according to the practical injection condition of 0.5 m/s in slow injection stage and 3.5 m/s in high injection stage.

Fig.4 shows the simulation results of mold filling

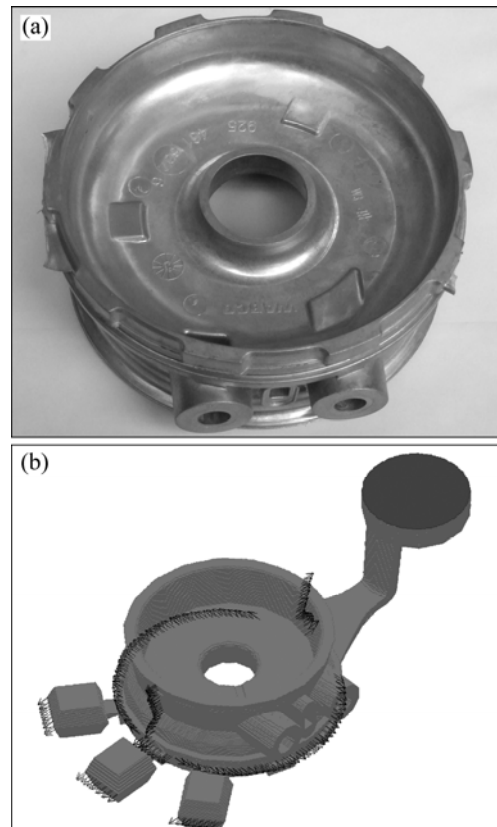


Fig.3 Practical high pressure die casting and setting of vents in simulation

Table 1 Thermal-physical data of casting and dies used in simulation

Material	Density/ (g·cm ⁻³)	Specific heat capacity/(J·g ⁻¹ ·°C ⁻¹)	Liquidus/ °C	Solidus/ °C	Heat conductivity/ (J ⁻¹ ·cm ⁻¹ ·s ⁻¹ ·°C ⁻¹)	Latent heat/ (J·g ⁻¹)	Initial temperature/°C
ADC1 (casting)	2.660	0.230	590	560	0.270	392.9	700
H13 (die)	7.800	0.543	—	—	0.272	—	200

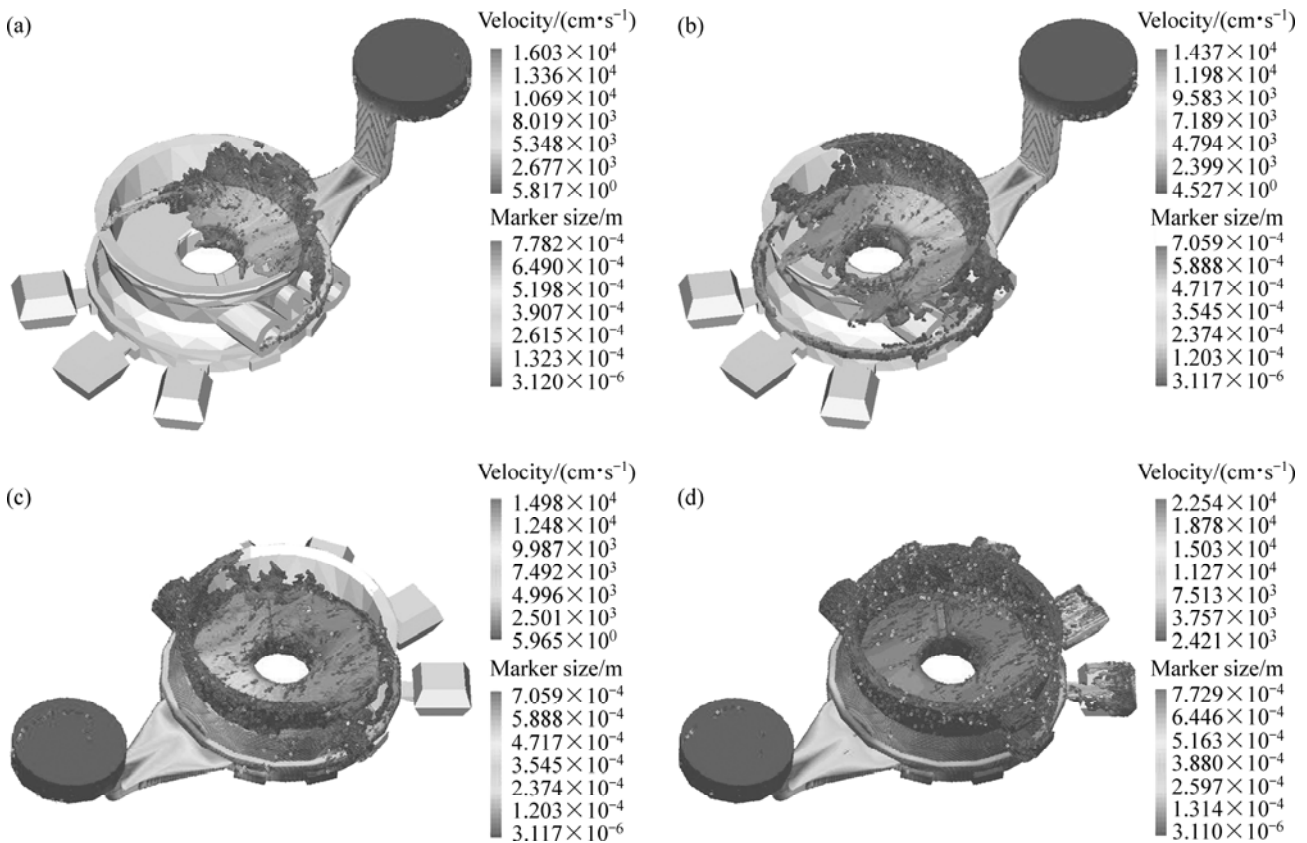


Fig.4 Simulation results of mold filling and gas entrapment of die casting: (a) 0.011 s; (b) 0.013 s; (c) 0.015 s; (d) 0.024 s

and gas entrapment. In the figure, different colors of the flowing melt express velocity; the markers indicate the entrapped gas with different sizes and the arrows attached to them illustrate flow direction of the entrapped gases. As shown in Fig.4(a), after the liquids passing through the ingate, major liquids flow to the up part and other liquids move along the circumference at the bottom part. Due to liquid slip on die wall with lubricant considered in this simulation, the liquids flowing along the circumference has higher velocity. They arrive at the entrance of the gates between the casting body and the overflow 0.013 s after injection as shown in Fig.4(b). Since they have high flow velocities along the direction of the circumference and the gates are thin, they meet together at the location of six o'clock (if defining the central of the ingate exit as twelve o'clock) rather than enter the overflows. These fluids seal with the gate entrance, which prevents from the cavity gas flowing out through the overflows. Fig.4(c) indicates that 0.015 s after the injection spraying flow of the liquids takes place at four o'clock location, which should result in the gas entrapment and final porosities. As can be seen in Fig.4(d), the liquids fill into the overflows after the casting body is fully filled.

Fig.5 displays the simulated results of temperature contours and gas entrapment after the die cavity filling

process. The part A has few entrapped gas. In contrast, a lot of cavity gases are entrapped into the part C. Fig.6 shows the temperature distribution contours during the casting solidification process, which indicate that the part A solidifies firstly and the part C has the longest solidification time among three parts.

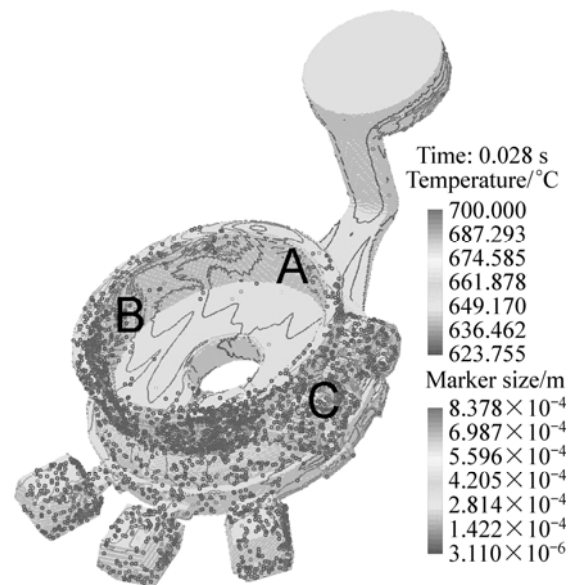


Fig.5 Simulation results of temperature distribution contour and gas entrapment after the filling process

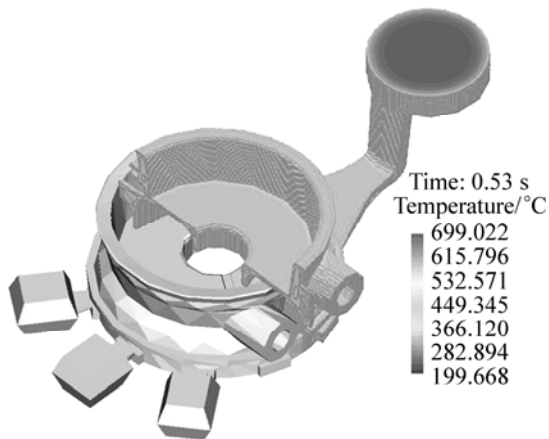


Fig.6 Simulated temperature field contours during casting solidification

3.2 Experimental validation

Since the proposed mold filling model have been validated with the in-situ X-ray observation in former research[13–14], the following part mainly focuses on comparison and validation of the porosity prediction. In the experiment, a practical die casting was cut at the parts A, B and C along the cylindrically rotational section. Figs.7(a) and 7(b) show the macro morphology of sections in the parts A and C, while Figs.7(c) and (d) show the details of the rectangles 1 and 2 in Fig.7(b) respectively at high magnification. It is obvious that no

macro-scale porosity is found in the part A and the porosities up to millimeter size can be clearly observed in the part C. This is in acceptable well agreement with the simulation results in Fig.5.

Three samples were obtained from the three parts respectively, and they were polished with fine sandpapers and then etched with a reagent of 1% HF. Their microstructures were observed and recorded with a Leica microscope, which are shown in Fig.8. Furthermore, the maximum porosity size in each sample was quantitatively analyzed with a digital analysis system conjunction with the microscope. Table 2 lists the comparison of experimental and simulated maximum porosity size in each part. The final porosity sizes are less than the predicted entrapped gases because the entrapped gases should shrinkage under high pressure near to 100 MPa from the main punch during the solidification process. Since the parts A and B solidified earlier, the high pressure can be efficiently transferred to the parts A and B from the punch. As a consequence, the final maximum porosity sizes in the two parts are no more than half of the predicted entrapped gases, and also the porosities are near spherical shape there. By contrast, the part C solidifies latterly and the pressure transfer is hindered due to the ingate solidification. This could be reason that in the part C the final maximum porosity size is about 60% as the original size of the predicted entrapped gas. The above comparison and discussion

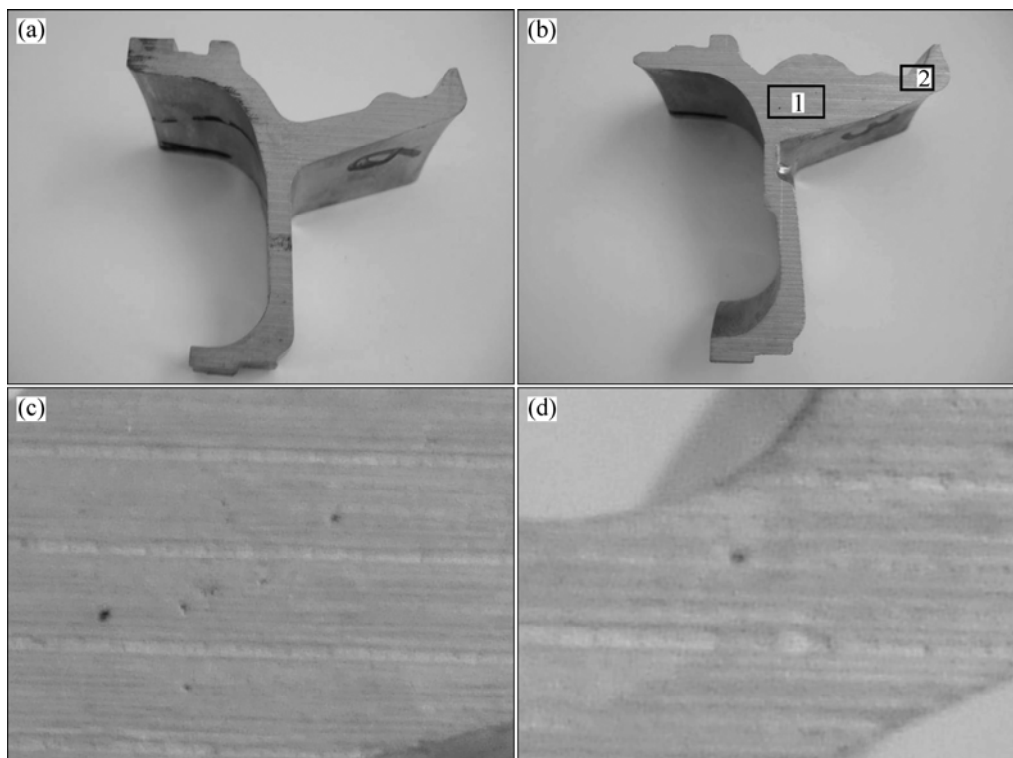


Fig.7 Morphologies of sections in parts A and C (refer to Fig.5): (a) Section of part A; (b) Section of part C; (c) Zoomed view of rectangle 1; (d) Zoomed view of rectangle 2

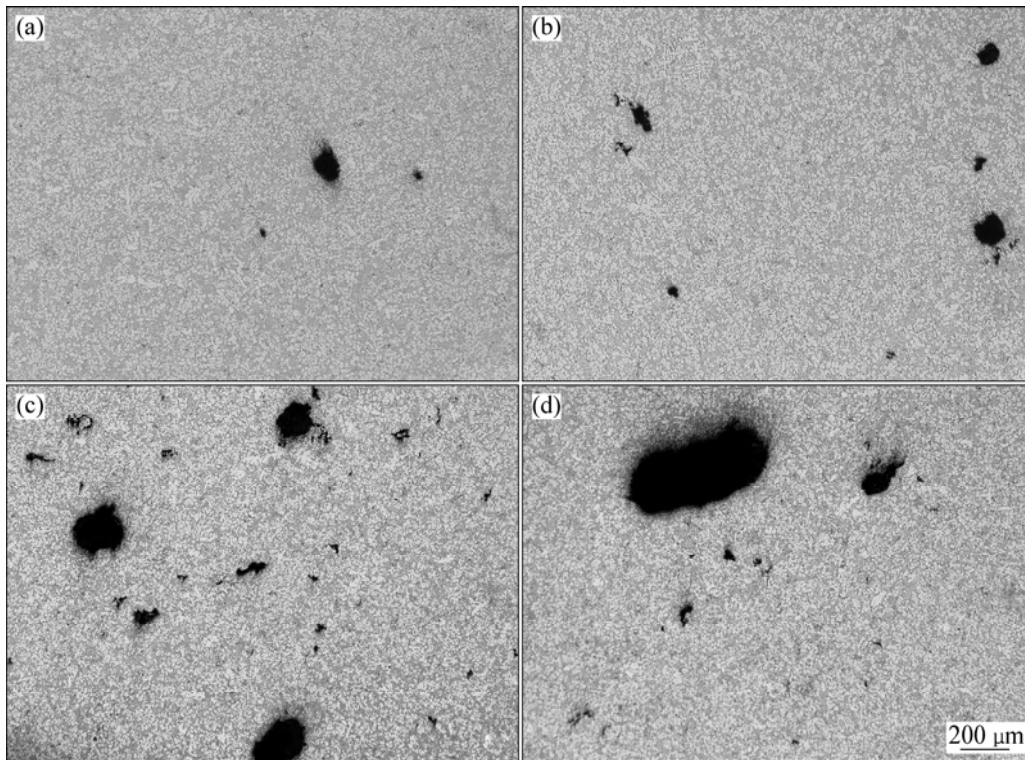


Fig.8 Metallurgical photos of samples: (a) Part A; (b) Part B; (c, d) Part C

demonstrate that the current simulation method is valid and can provide useful information for process analysis and optimization of practical high pressure die castings. It is interesting to note that there exist several shrinkage micro-porosities among the big porosities resulting from the entrapped gases in Fig.8(c). This is coinciding with the results in AM50 high pressure die castings reported by LEE[15]. In his viewpoint, entrapped gases should decrease heat transfer during solidification process and may induce new hotspots among them, resulting in the so-called gas induced shrinkage porosities.

Table 2 Comparison of experimental and predicted maximum porosity size in parts A, B and C in Fig.5

Location in Fig.5	Predicted/ μm	Experimental/ μm
A	220	94
B	420	162
C	640	375

4 Conclusions

1) The mathematical model of mold filling and gas entrapment for die casting process were established. It was applied to the practical high pressure die casting. The simulation results were compared with the experimental analysis. The application confirms the validity of the proposed method in location and qualitative size of predicted entrapped gas.

2) The study shows that efficient pressure from main punch can compress entrapped gases during solidification process, and thus early-solidified parts have small and near-spherical porosities. It is concluded that gas porosity sizes in high pressure die castings are dependent on both gas entrapment during mold filling and pressure transfer within the solidification period as well.

References

- [1] LEE S G, GOKHALE A M, PATEL G R, EVANS M. Effect of process parameters on porosity distribution in high-pressure die-cast AM50 Mg alloy [J]. *Materials Science and Engineering A*, 2006, 427: 99–111.
- [2] HU H, ZHOU M, SUN Z Z, LI N. Tensile behavior and fracture characteristics of die cast magnesium alloy AM50 [J]. *Journal of Materials Processing Technology*, 2008, 201: 364–368.
- [3] SONG J, XIONG S M, LI M, ALLISON J. The correlation between microstructure and mechanical properties of high-pressure die-cast AM50 alloy [J]. *Journal of Alloys and Compounds*, 2009, 477: 863–869.
- [4] AGHION E, MOSCOVITCH N, ARNON A. The correlation between wall thickness and properties of HPDC magnesium alloys [J]. *Materials Science and Engineering A*, 2007, 447: 341–346.
- [5] WEILER J P, WOOD J T, KLASSEN R J, MAIRE E, BERKMORTEL R, WANG G. Relationship between internal porosity and fracture strength of die-cast magnesium AM60B alloy [J]. *Materials Science and Engineering A*, 2005, 395: 315–322.
- [6] BREVICK J R. Die casting defects causing rejections during machining [J]. *Die Casting Engineer*, 1997, 5: 42–46.

- [7] McLAUGHLIN M, KIM, C W, CONARD A. An application of trapped-air analysis to large, complex, high-pressure magnesium casting [J]. *Die Casting Engineer*, 2004, 9: 40–45.
- [8] KIMATSUKA A, OHNAKA I, ZHU J D, KAMITSU T. Mold filling simulation with consideration of gas escape through sand mold [J]. *International Journal of Cast Metals Research*, 2002, 15 : 149–152.
- [9] KIMATSUKA A, OHNAKA I, ZHU J D, OHMACHI T. Mold filling simulation of high pressure die casting for predicting gas porosity [C]//STEFANESCU D, WARREN J, JOLLY M, KRANE M, ed. *Modeling of Casting, Welding and Advanced Solidification Processes*. Danvers, USA: TMS, 2003: 335–342.
- [10] SAKURAGI T. Prediction of gas hole by mold-filling simulation with consideration of surface tension [J]. *JSME International Journal B—Fluids and Thermal Engineering*, 2004, 47: 699–708.
- [11] ZHAO H D, WANG F, LI Y Y, XIA W. Experimental and numerical analysis of gas entrapment defects in plate ADC12 die castings [J]. *Journal of Materials Processing Technology*, 2009, 209: 4537–4542.
- [12] ZHU J D, OHNAKA I. Three dimensional computer simulation on mold filling of casting by direct finite difference method [J]. *Journal of Japanese Foundry Engineering*, 1996, 68: 668–676.
- [13] ZHAO H D, OHNAKA I, ZHU J D. Modeling of mold filling of Al gravity casting and validation with X-ray in-situ observation [J]. *Applied Mathematical Modelling*, 2008, 32: 185–194.
- [14] ZHAO H D, OHNAKA I. Numerical simulation of oxide entrapment and mold filling process of Al casting [J]. *The Chinese Journal of Nonferrous Metals*, 2005, 15: 1200–1207. (in Chinese)
- [15] LEE S G, GOKHALE A M. Formation of gas induces shrinkage porosity in Mg-alloy high-pressure die-castings [J]. *Scripta Materialia*, 2006, 55: 387–390.

(Edited by LAI Hai-hui)